

## Article

# Micromagnetic Properties of Powder Metallurgically Produced Al Composites as a Fundamental Study for Additive Manufacturing

Maraike Gräbner <sup>1,\*</sup>, Henning Wiche <sup>1</sup>, Kai Treutler <sup>2</sup>  and Volker Wesling <sup>2,\*</sup>

<sup>1</sup> Clausthaler Zentrum für Materialtechni (CZM), Clausthal University of Technology, 38678 Clausthal-Zellerfeld, Germany; henning.wiche@tu-clausthal.de

<sup>2</sup> Institute of Welding and Machining (ISAF), Clausthal University of Technology, 38678 Clausthal-Zellerfeld, Germany; kai.treutler@tu-clausthal.de

\* Correspondence: maraike.graebner@tu-clausthal.de (M.G.); office@isaf.tu-clausthal.de (V.W.)

**Featured Application:** Detection of stresses or stress peaks and potentially aging processes in the device.

**Abstract:** Resource-efficient manufacturing with a high degree of freedom in terms of component shape can be realised through additive manufacturing. The focus can lie not only on the manufacturing process in terms of geometrical correctness, stability, etc., but also on the targeted development of specific material properties. This study shows the development of hybrid material systems made of aluminium and the ferromagnetic particles iron, cobalt, and nickel. The aim is to use the ferromagnetic properties as sensor properties to enable the easy sensing of material properties such as the microstructure, fatigue, or occurring stresses. To easily adopt different compositions, hot isostatic pressing was selected for the characterisation of the material composites Al-Fe, Al-Ni, and Al-Co with regard to their magnetic properties. Subsequently, transfer to the additive manufacturing process of wire and arc additive manufacturing gas metal arc welding was carried out by mixing the powder separately into the weld pool. The study shows that it is possible to prevent a complete transformation of Ni and Co into intermetallic phases with Al by adjusting the influencing variables in the HIP process. Magnetic properties could be detected in the composites of Al-Co and Al-Fe. This work serves as a preliminary work to realise additive components made of hybrid material systems of Al-Fe, Al-Co, and Al-Ni with the GMA welding process.

**Keywords:** magnetic properties; hybrid system; sensor properties



**Citation:** Gräbner, M.; Wiche, H.; Treutler, K.; Wesling, V. Micromagnetic Properties of Powder Metallurgically Produced Al Composites as a Fundamental Study for Additive Manufacturing. *Appl. Sci.* **2022**, *12*, 6695. <https://doi.org/10.3390/app12136695>

Academic Editor: Manoj Gupta

Received: 31 May 2022

Accepted: 29 June 2022

Published: 1 July 2022

**Publisher's Note:** MDPI stays neutral with regard to jurisdictional claims in published maps and institutional affiliations.



**Copyright:** © 2022 by the authors. Licensee MDPI, Basel, Switzerland. This article is an open access article distributed under the terms and conditions of the Creative Commons Attribution (CC BY) license (<https://creativecommons.org/licenses/by/4.0/>).

## 1. Introduction

The development of material properties deals, on the one hand, with the modification and, on the other hand, with the control of the macrostructure and the microstructure. This study focuses on the control of the microstructure of a pseudo-alloy. The microstructure of a metal is related not only to its mechanical properties, but also to its magnetic properties. If modification or damage occurs in the microstructure, this inevitably leads to deviating magnetic properties. This link should serve as a foundation for the use of ferromagnetic material properties as sensor properties [1].

Aluminium is weakly paramagnetic, but compared with ferromagnetic materials such as cobalt (Co), iron (Fe), and nickel (Ni), it can be defined as nonmagnetic. The aim of this study is to implant the nonmagnetic material Al with ferromagnetic particles iron (Fe), cobalt (Co), and nickel (Ni). In these materials, regions with identical magnetisation directions, which are called magnetic domains, are characteristic. Domains with different orientations are separated from each other by Bloch walls, see Figure 1a. The Bloch walls shift when a ferromagnetic material is exposed to an electromagnetic field. As a result

of the shift, the Bloch walls interact with defects such as grain boundaries, dislocations, or segregations, as, from an energetic point of view, it is more attractive to attach to the irregularities. This phenomenon, known as pinning of the Bloch walls, is illustrated in Figure 1b. The interaction of the Bloch walls with defects causes them to move abruptly when the external applied magnetic field provides enough energy for the walls to tear themselves away from the defects. This results in a constant change between tearing loose and pinning on a microscopic level, which Heinrich Barkhausen made audible in his experiment in 1919, after which the magnetic Barkhausen noise received its name. This method is used for micromagnetic material characterisation (MikroMach) to generate magnetic characteristic values of materials. Barkhausen noise analysis also offers the great advantage of being almost independent of the sensor head coupling [1–4].

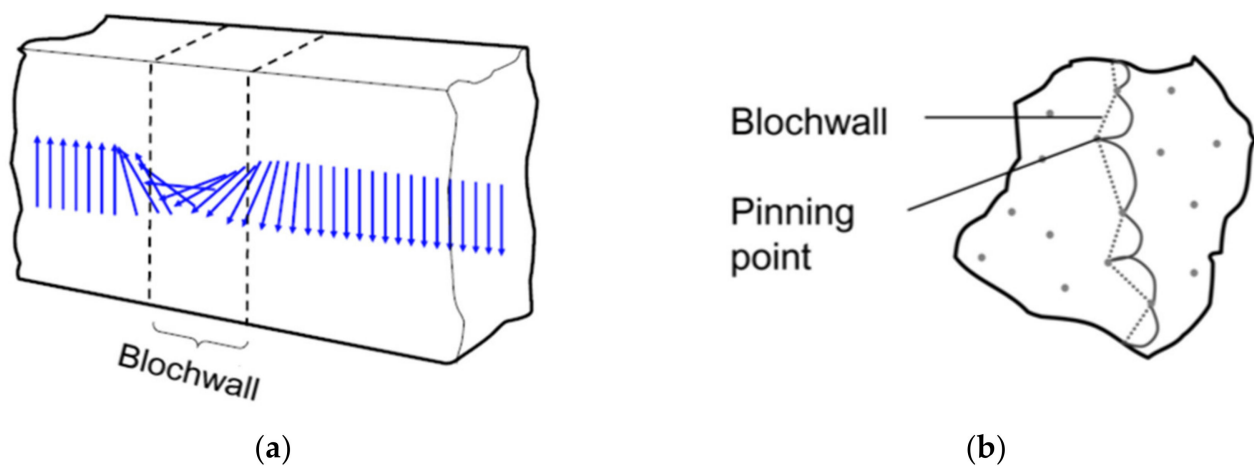


**Figure 1.** (a)  $180^\circ$  Bloch wall between two differently oriented domains and (b) pinned Bloch wall [5,6].

To characterise the material composite of Al with Fe, Co, and Ni, samples were generated by hot isostatic pressing (HIP). HIP enables the production of a homogeneous, compact material composite with isotropic material properties. Therefore, an almost “ideal” material behaviour can be realised for determination of the magnetic properties [7,8].

The HIP process with pure Al has already been explained in some studies, as well as for Al-Fe [9–12]. For nickel, the focus in the literature is on Ni superalloys and for Co on Co-chromium or Co-TiC alloys [13–15]. Otherwise, there are only reports on the melt-metallurgical production of all of the listed material composites [16,17]. The focus of other studies is the complete transformation of the material composites, such as [11,18], but not, as here, on the partial preservation of the particles to ensure ferromagnetic properties.

The following study serves as a preliminary work for the implementation of a hybrid material made of Al with Co, Ni, and Fe, which should be realised by an additive manufacturing process, f.e., wire and arc additive manufacturing. Compared with traditional processes, additive manufacturing offers a high degree of freedom in the production of complex and hybrid materials, allowing components to be produced in a resource-efficient way [19,20]. Consequently, the gas metal arc welding (GMAW) process was chosen for the welding implementation. In the literature, there are already studies on the connection of Al and Fe with laser welding, which are summarised in [21]. Al-Fe and Al-Ni can also be joined by magnetic pressure seam welding [22]. Cobalt is welded in compounds with other elements, for example laser welding of CoCr [23]. It is not obvious from the literature how to generate a material composite of Al-Ni and especially Al-Co by welding. A new approach of realising a material composite of Al-Fe, Al-Ni, and Al-Co by the GMA welding process is presented in this study by implementing the ferromagnetic particles directly into the weld pool.

## 2. Materials and Methods

For the realisation of a high filling density in the HIP capsule, Al, Fe, Co, and Ni are used in spherical powder form [24,25]. Al, Ni, and Fe have particle sizes of 45  $\mu\text{m}$  to 150  $\mu\text{m}$ . To integrate the influence of the particle size, a Co powder with a 300  $\mu\text{m}$  particle size was chosen. As the focus of the following investigations is on the ferromagnetic properties of the materials, the properties are listed in Table 1.

**Table 1.** Magnetic properties of Fe, Co, and Ni [26–29].

Material	Lattice Structure	Magnetic Permeability $\mu$	Saturation Polarisation $J_S$ [T]	Curie Temperature $T_C$ [ $^{\circ}\text{C}$ ]
Fe	bcc	250–680	2.15	1043
Co	hcp	80–200	1.76	1393
Ni	fcc	280–2500	0.61	631

First, the powders are mixed with a 3D shaker mixer for 1 h according to the composition in Table 2. Because HIP is only used for the characterisation of the Al-particle composites and in order not to eliminate the good deformation properties of Al, 10 mass-% of ferromagnetic particles were initially selected. As no magnetic feedback could be generated, 30 mass-% was subsequently selected. The 30 mass-% is the maximum percentage of magnetic particles, as even 10 mass-% significantly reduces the plastic deformation properties of the Al, which this study verifies. The 3D shaker mixer achieves effective mixing of the powders through the interaction of rotation, translation, and inversion during the mixing process. The powder is filled into stainless steel HIP containers, precompacted, evacuated, and sealed. An HIP system essentially consists of an insulating jacket, a furnace, and a pressure chamber, see Figure 2a. Up to three hip capsules are placed in the HIP chamber, and after sealing, it is flooded with argon. Surrounded by this inert gas atmosphere, the capsules are heated to 500  $^{\circ}\text{C}$ , whereby the pressure increases because of heating, see Figure 2b, and they act uniformly on the entire outside of the capsule to ensure compression over the entire cross-section. A pressure of 1200 bar was selected for test numbers one to four, and 1100 Pa was selected for test numbers five to seven. After the heating phase, the temperature and pressure are kept constant for 3 h, and then the cooling phase begins. After HIP, the specimens have a diameter of 50 mm and a height of 100 mm, with the cover and base removed because of deformation [30,31].

**Table 2.** Material composition of the hiped samples.

Test Number	Material	Mass Fractions [%]
1	Al	100
2	Al Fe	90 10
3	Al Co	90 10
4	Al Ni	90 10
5	Al Fe	70 30
6	Al Ni	70 30
7	Al Co	70 30

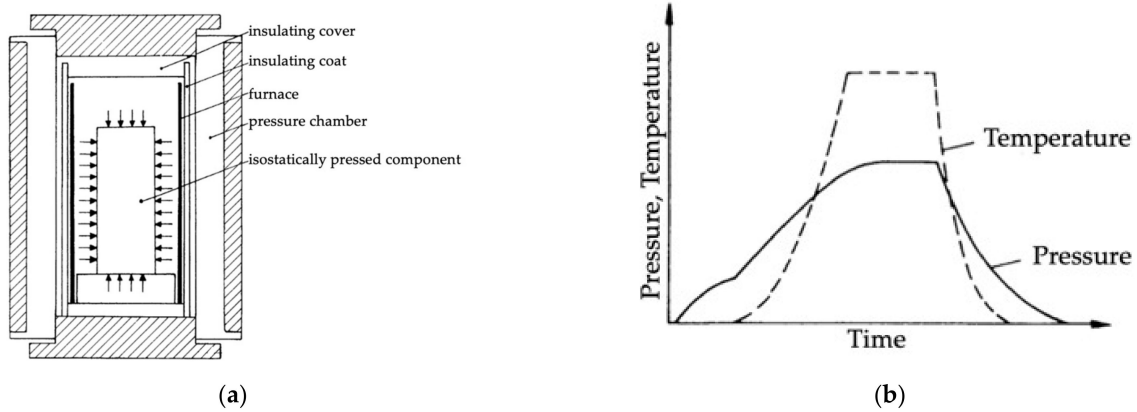


**Figure 2.** (a) Pressure chamber of the HIP system and (b) pressure and temperature curve as a function of time [30].

The microstructure and magnetic properties of the resulting hipped materials are examined for their magnetic properties. Barkhausen noise analysis is used for the detection of the magnetic characteristics. The Barkhausen noise analysis detects the jumps in magnetisation caused by the irreversible Bloch walls movement from the 180° Bloch walls. To induce Bloch wall jumps, the material is subjected to time-periodic remagnetisation, whereby a ferromagnetic material passes through a hysteresis process, see Figure 3a. The abrupt changes in magnetisation induce voltage pulses in the magneto-inductive sensor, which is located in the testing head of the measuring instrument, see Figure 3b. The testing head is placed on the material surface and acts as a transmitter and receiver of the magnetic signals. MikroMach allows a Barkhausen noise profile curve to be plotted, as in Figure 3a, with the voltage pulses being most extensive around the coercive field strength  $H_C$ . For the measurements, samples with the shape shown in Figure 4a were eroded from the material produced by HIP, then, the erosion layer was removed, and the Barkhausen noise curve was recorded at a magnetisation frequency of 55 Hz and a magnetisation amplitude of 70 A/cm. The testing head could be placed vertically on the surface using the setup shown in Figure 4b [2,4].

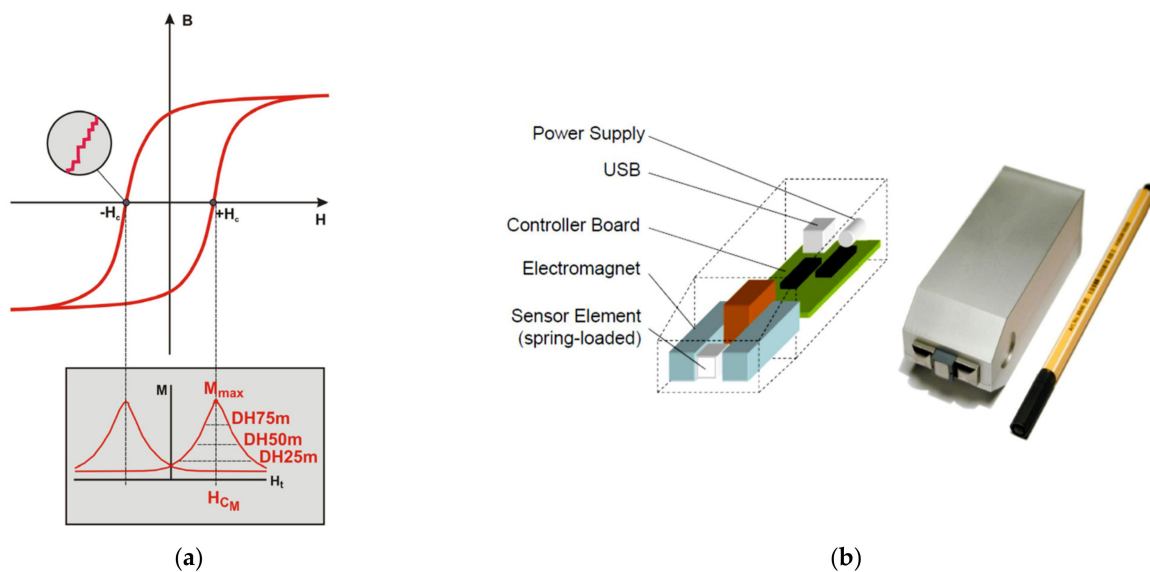


**Figure 3.** (a) Barkhausen noise profile curve in connection with the hysteresis curve and (b) MikroMach sensor construction [4,32].

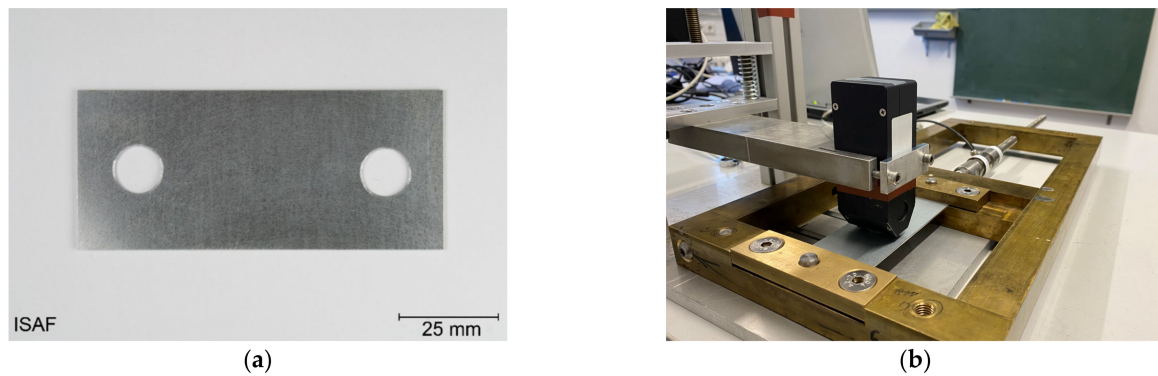


**Figure 4.** (a) Sample form for measuring magnetic properties and the (b) testing device.

In addition to the microstructure and the magnetic properties, the mechanical properties of the HIP samples are another focus of the investigations. To determine the mechanical properties, the tensile test was carried out in accordance with DIN EN ISO 6892-1. Specimen shape A with cylindrical specimen heads and a diameter of 4 mm was selected in reference to DIN 50125. To remove the tensile specimens from the HIP specimens, cylindrical bars were eroded from the material and then shaped into the desired final form on the lathe. For the tensile test, the control mode deformation was selected at a speed of 0.48 mm/min. A fine strain extensometer was used, which was removed at 1% strain.

After the material combinations of Al with the Fe, Co, and Ni particles were characterised by HIP, the welding realisation followed on the basis of the results by a GMA-welding process with the Fe powder. The nonmagnetic component is an AlMg3 welding wire with a diameter of 1.2 mm, whose composition is listed in Table 3. The welding wire is melted, and the ferromagnetic particles are implemented in the molten bath through an additional feed line, see Figure 5. Here, it is elementary to add the particles behind the arc to ensure a lower energy input and to prevent intermetallic phase formation. The selected process parameters are shown in Table 4. The particles and wire did not receive any preheating and were introduced into the process at room temperature. The AlMg3 wire was deposited onto an Al plate, which was not preheated either. The particles enter the AlMg3 melt pool through a powder inlet that was placed at a  $67^\circ$  angle to the Al plate.

**Table 3.** Composition of the welding wire AlMg3 [33].

Element	Al	Mg	Mn	Cr	Ti
Mass fractions [%]	basis	3.00	0.30	0.10	0.13



**Figure 5.** Process setup for the admixture of the magnetic powders in the weld pool.

**Table 4.** Process influencing the variables of the GMAW process.

Process		Puls
Protective gas		argon
Forward speed of torch	[cm/min]	30.00
Forward speed of wire [m/min]	[m/min]	9.50
Voltage	[V]	21.50
Current	[A]	152.00
Gas supply	[L/min]	4.00
Powder supply	[g/min]	60.00

### 3. Results

In the following, the results of the material characterisation based on the HIP process are firstly described. The microstructure and the mechanical and magnetic properties are the focus of the investigations. Finally, an idea for the welding implementation is presented.

#### 3.1. HIP

##### 3.1.1. Microstructure

The metallographic preparation of the samples was divided into the following steps: grinding with SiC abrasive paper of various grit sizes, polishing with diamond paste of various grit sizes, and recording of the microstructural images using a Leica DM6M microscope. The pure Al was etched four times for 30 s with Barker after polishing, and then the microstructure was recorded with polarised light. The unetched microstructure of the Al-particle composite was visualised using bright field microscopy. A nearly homogeneous, globular grain structure could be created in the pure Al by HIP, see Figure 6a. The magnetic particles Co, Ni, and Fe could be implemented homogeneously into the Al matrix, see Figure 6b, where the formation of intermetallic phases occurred. The reaction between Al and Co resulted in an intermetallic phase seam around the pure particles, see Figure 6c, for Ni, and two phase seams appeared, see Figure 6d. Compared with Co and Ni, Fe has a stronger tendency to form an intermetallic phase with Al because the whole particle is changed, see Figure 6e,f. Ni and Co develop the same phase seams for 10 mass-% and 30 mass-%, while Fe develops different phases. For the characterisation of the respective intermetallic phases, an EDX mapping analysis with a Helios Nanolab 600 was carried out to analyse the distribution of the elements in the Al and particle transition area. The investigations were conducted under a high vacuum, and an accelerating voltage of 15.0 kV and a beam current of 1.4 nA were used. A working distance of 5.1 mm was selected for Al with Co particles, 4.7 mm for Fe, and 6.0 mm for Ni. The findings for the Co particle, for example, are shown in Figure 7. As a result of the measured components, an intermetallic phase with the composition  $Al_9Co_2$  was formed around the pure Co particle. Ni forms  $Al_3Ni$  on the outside and  $Al_3Ni_2$  on the inside around the pure Ni particle. The 10 mass-% Fe led to the formation of  $Al_{13}Fe_4$  phases. Further investigations are currently being conducted for the phase determination of the 30 mass-%, but the microstructural images in Figure 6f indicate that a different phase was formed.

##### 3.1.2. Mechanical Properties

The averaged mechanical properties from three tensile tests and the associated standard deviations are represented in Figure 8. Compared with pure Al, the addition of 10 mass-% and 30 mass-% Fe and Ni leads to an increase in tensile strength as well as yield strength, see Figure 8a,b. In comparison, the composite of Al and Co has a low tensile strength. The addition of 10 mass-% Co leads to a higher yield strength, at 30 mass-%, it has similar values as the pure Al. The plastic deformability decreases with the addition of the magnetic particles, where 10 mass-% Co and Ni show the highest values, see Figure 8c,d.

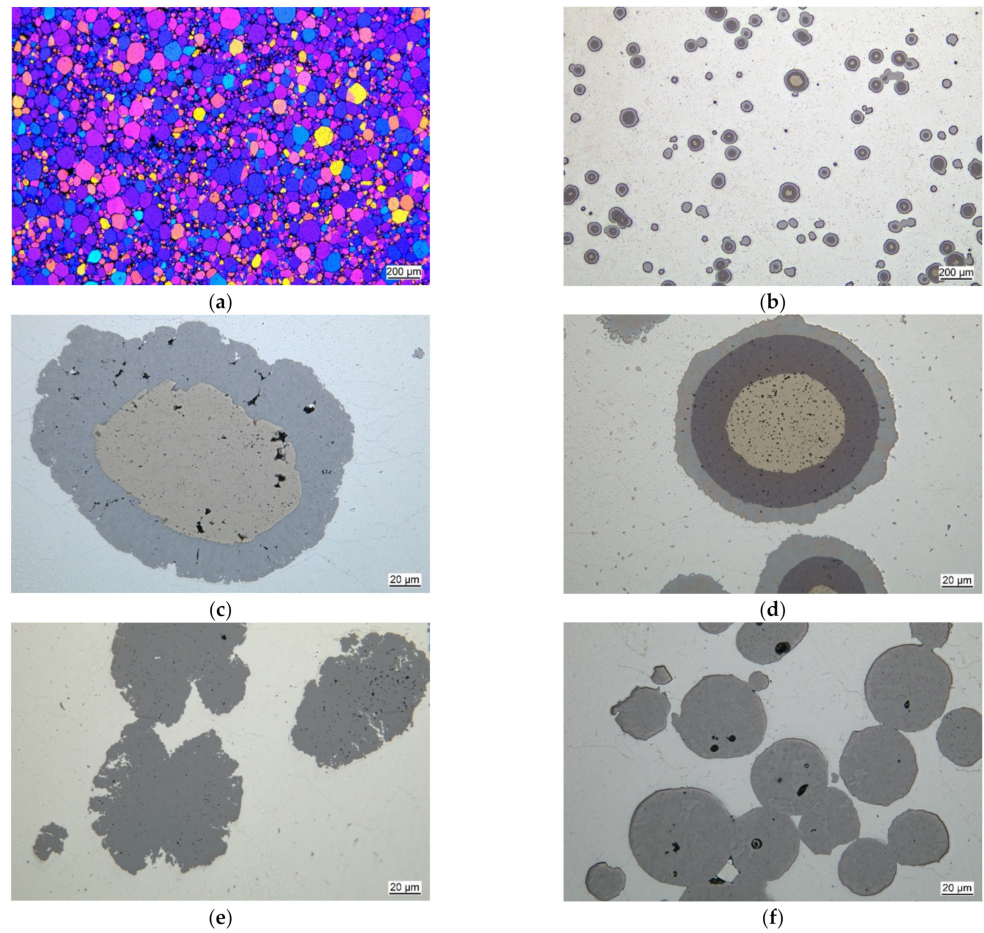


**Figure 6.** Images of the different microstructures through a reflected light microscope of (a) Al and Al-matrix with 10 mass-% for (b) Ni-, (c) Co-, (d) Ni-, and (e) Fe-particles, and (f) Al-matrix with 30 mass-% Fe.

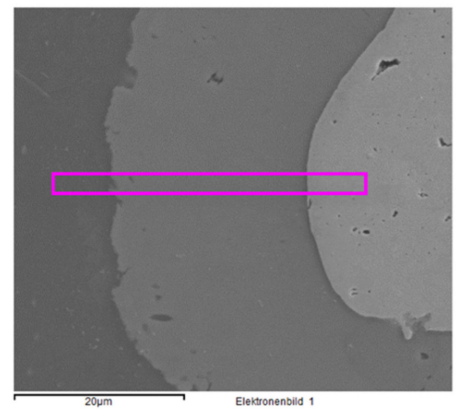
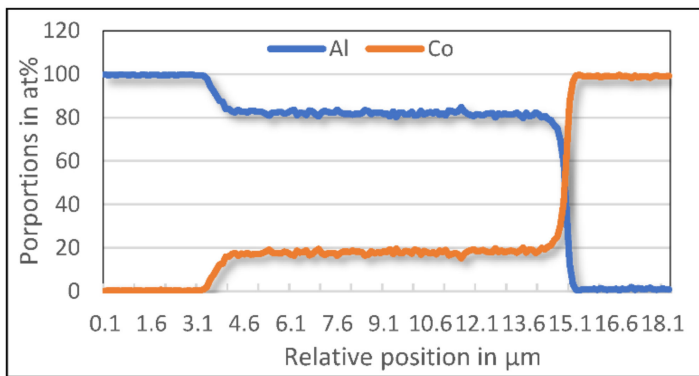


**Figure 7.** EDX analysis of the Al matrix with 10 mass-% Co: (a) EDX mapping showing the distribution of the elemental composition over the selected range, see (b). EDX mapping indicates that a Co and Al phase has formed in the transition region.

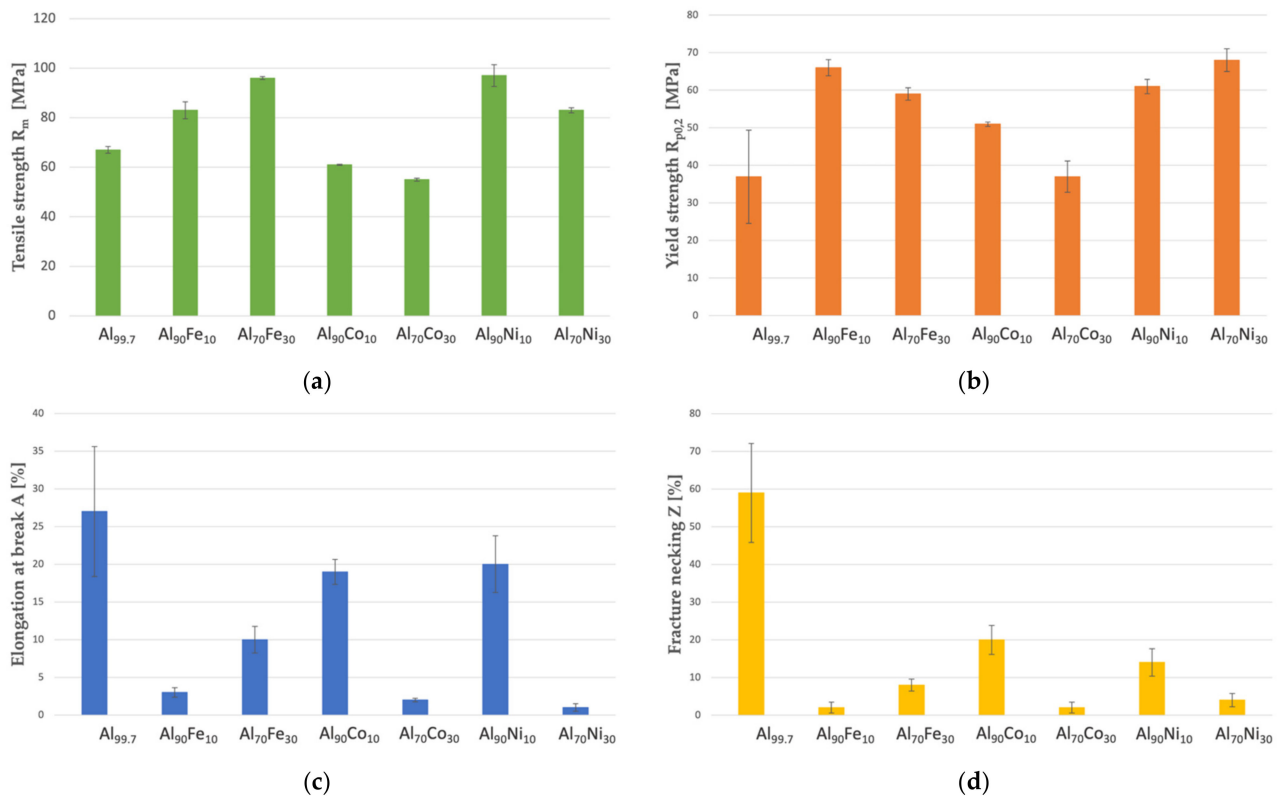


**Figure 8.** Characteristic values of the tensile test of pure Al and Al composite with different proportions of magnetic particles: (a) tensile strength, (b) yield strength, (c) elongation at break, and (d) fracture necking.

The mechanical properties varied strongly as a function of the mass-%. The increase from 10 mass % to 30 mass-% shows no classified behaviour. With Fe, the tensile stress and the plastic deformation capacity are increased, but the yield strength is decreased. Co leads to a lowering of all mechanical properties. Increasing the Ni content decreases the tensile stress and plastic deformability, while increasing the yield strength. For illustration purposes, a selected stress-strain curve of each material is shown in Figure 9.

### 3.1.3. Magnetic Properties

Pure Al is nonmagnetic, which is confirmed by the measurements that have been carried out with MikroMach. The addition of 10 mass-% is not sufficient to obtain magnetic feedback from the material. In contrast, magnetic characteristic values can actually be determined with 30 mass-% Fe and Co. For illustration, the characteristic value  $M_{max}$  of the Barkhausen noise analysis is shown in Figure 10. The higher the characteristic value  $M_{max}$  is, the more Bloch wall displacements take place on the basis of the existence of magnetic domains. Accordingly, it was possible to generate an Al composite with magnetic properties, on the one hand, due to the selective preservation of the Co particle and, on the other hand, due to a magnetic, intermetallic phase of Al and Fe.

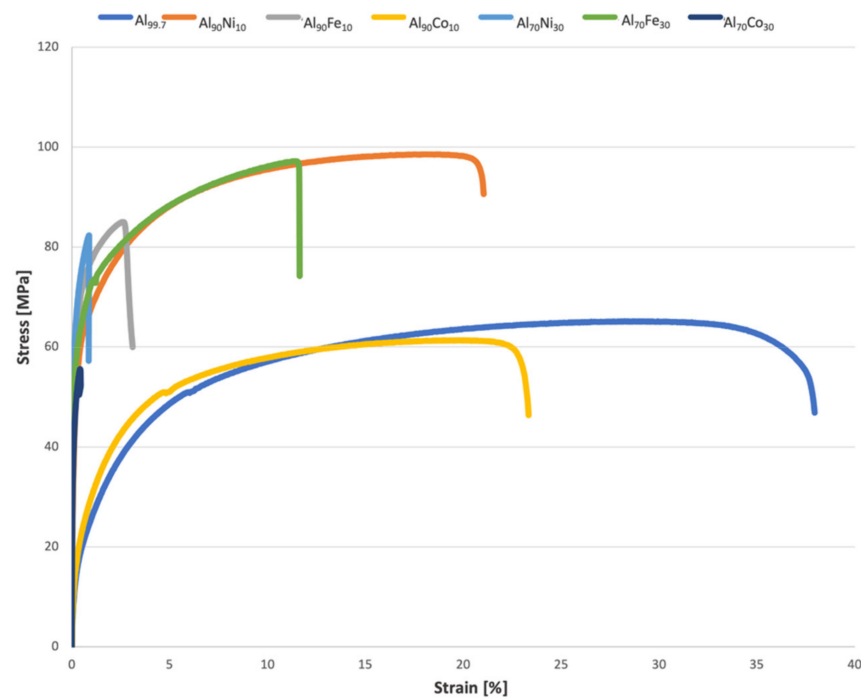


**Figure 9.** Stress-strain diagram of Al and Al with different percentages of ferromagnetic particles Fe, Ni, and Co.

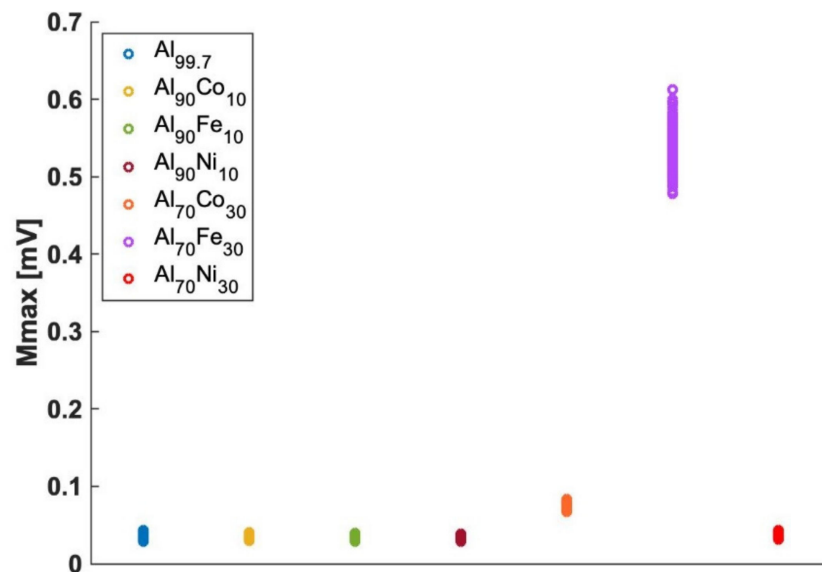


**Figure 10.** Characteristic value Mmax of the Barkhausen noise analysis for the hybrid materials, whereby magnetic feedback could be deactivated by the addition of 30 mass-% Fe and Co.

### 3.2. Welding Implantation

The finding from the previous HIP process is that Fe is the most promising element for generating a sensor property based on a ferromagnetic character. The implementation of pure Fe, Co, and Ni in the molten bath also resulted in the formation of an intermetallic phase, see Figure 11, which did not show any magnetic properties in the MikroMach measurement. The intermetallic phase of Al and Fe is quite homogeneously distributed, see Figure 11. Co and Ni form larger intermetallic phase areas that are also found throughout the weld. In addition to the microstructure, the phase fractions in the weld beads were investigated metallographically. The phase fraction was found to be 24 % Fe, 14 % Co, and

26 % Ni. Fe had a smaller fractionation with 45  $\mu\text{m}$  to 150  $\mu\text{m}$  compared with Co with 300  $\mu\text{m}$ , resulting in a finer distribution in the weld pool, see Figure 11.

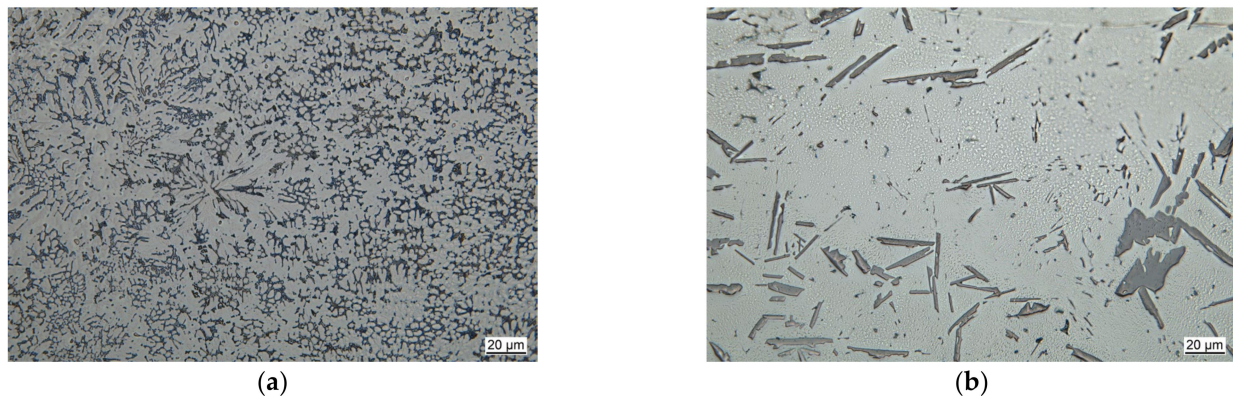


**Figure 11.** Weld bead of AlMg3 with (a) Fe particles and (b) Co particles.

#### 4. Discussion

The HIP process shows that the implementation of magnetic particles in an Al matrix makes it possible to use the ferromagnetic properties as sensing properties. Here, Fe and Co proved to be the most promising elements. The Co particle has the least tendency to form an intermetallic phase because the phase seam is smaller compared with Ni. Fe reacts with Al to form a complete intermetallic phase. In terms of magnetic properties, the study shows that it is not exclusively the maintenance of the pure particle that is targeted, but also the generation of intermetallic magnetic phases. From the mechanical properties obtained, a complete implementation of the Al material is not efficient as these lead to a significant reduction in plastic deformability from 30% by mass. Consequently, it is desirable to partially integrate the particles into the Al component. The realisation and determination of the magnetic properties with selective implementation of the particles are the focus of further investigations. In addition, the dependence of the magnetic properties on an applied stress state should be determined for this hybrid material combination. For the application of the selected material systems as sensors, it should be ensured that the magnetic characteristic values change through variation of the stress states. The correlation of the magnetic properties with the microstructure is discussed in this study to the point that different magnetic properties can be determined as a function of the particles. The change in magnetic properties due to microstructural modifications will be considered in further investigations.

The welding implementation simply provides the basis for further investigations. A positive aspect is the homogeneous distribution of the intermetallic phases in the molten bath. The process setup actually offers the possibility of introducing ferromagnetic particles into the weld pool. The focus of further investigation is the dependence of the magnetic feedback of the weld beads on the distribution of the phases, their composition, and the cooling conditions. The aim is to ensure a controlled addition of specific mass-% of particles and to be able to use the ferromagnetic properties of an Al-Fe composite produced by the GMAW process as sensor properties.

#### 5. Conclusions

The study has shown that it is possible to create a hybrid material system consisting of Al and ferromagnetic particles. The composites of Al-Fe, Al-Co, and Al-Ni were characterised by HIP, with a focus on the microstructure and the mechanical and magnetic properties. The avoidance of a completely formed intermetallic phase in the Al-Co and Al-Ni composites by the adjusted Hip process parameters is to be emphasised. In addition, Fe proved to be the most promising component for detecting ferromagnetic properties. Regarding additive manufacturing of the material composite of Al and Fe, an approach

was created to realise this material combination by a GMA welding process. Depending on the particles, a different phase was established in the weld pool.

**Author Contributions:** Conceptualization, M.G. and H.W.; methodology, M.G. and H.W.; software, M.G.; validation, M.G.; formal analysis, M.G.; investigation, M.G.; resources, H.W.; data curation, M.G.; writing—original draft preparation, M.G.; writing—review and editing, H.W. and K.T.; visualization, M.G.; supervision, V.W.; project administration, V.W.; funding acquisition, H.W. and K.T. All authors have read and agreed to the published version of the manuscript.

**Funding:** Funded by the Ministry for Science and Culture of Lower Saxony (MWK), School for Additive Manufacturing SAM (78904-63-3/19).

**Data Availability Statement:** The data are available upon request.

**Acknowledgments:** We acknowledge the support of the Open Access Publishing Fund of Clausthal University of Technology. We also acknowledge the support of the Centre for Materials Engineering of Clausthal and, in particular, René Gustus.

**Conflicts of Interest:** The authors declare no conflict of interest.

## References

1. Ostermann, F. *Anwendungstechnologie Aluminium*; Springer: Berlin/Heidelberg, Germany, 2014.
2. Szielasko, K. Entwicklung Messtechnischer Module zur Mehrparametrischen Elektromagnetischen Werkstoffcharakterisierung Und-Prüfung. Ph.D. Thesis, Universität des Saarlandes, Saarbrücken, Germany, 2009.
3. Barkhausen, H. Zwei mit Hilfe der neuen Verstärker entdeckte Erscheinungen, *Physikalische Zeitschrift. Phys. Z.* **1919**, *20*, 401–403.
4. Tschuncky, R. Sensor-und Geräteunabhängige Kalibrierung Elektromagnetischer Zerstörungsfreier Prüfverfahren zur Praxisorientierten Werkstoffcharakterisierung. Ph.D. Thesis, Universität des Saarlandes, Saarbrücken, Germany, 2011.
5. Boller, C.; Alpeter, I.; Dobmann, G.; Rabung, J.; Schreiber, J.; Szielasko, K.; Tschuncky, R. Electromagnetism as a means for understanding materials mechanics phenomena in magnetic materials. *Mater. Werkst.* **2011**, *42*, 269–278. [[CrossRef](#)]
6. 14.03.2014; Versuch MagMat: Magnetische Eigenschaften der Materialien (IGP). Institut für Werkstofftechnik: Ilmenau, Germany, 2014.
7. Romero, A.; Morales, A.; Herranz, G. Enhancing Properties of Soft Magnetic Materials: A Study into Hot Isostatic Pressing and Sintering Atmosphere Influences. *Metals* **2021**, *11*, 643. [[CrossRef](#)]
8. Ma, J.; Qin, M.; Zhang, L.; Tian, L.; Ding, X.; Qu, X. Improvements in magnetic performance and sintered density of metal injection-molded soft magnetic alloy by hot isostatic pressing. *Mater. Lett.* **2014**, *125*, 227–230. [[CrossRef](#)]
9. Atkins, H.; Davies, S. Fundamental Aspects of Hot Isostatic Pressing: An Overview. *Metall. Mater. Trans. A* **2000**, *31*, 2981–3000. [[CrossRef](#)]
10. Bocanegra-Bernal, M.H. Review—Hot Isostatic Pressing (HIP) technology and its applications to metals and ceramics. *J. Mater. Sci.* **2004**, *39*, 6399–6420. [[CrossRef](#)]
11. Rabin, B.H.; Wright, R.N. Microstructure and Tensile Properties of Fe<sub>3</sub>Al Produced by Combustion Synthesis/Hot Isostatic Pressing. *Metall. Trans. A* **1992**, *32*, 35–40. [[CrossRef](#)]
12. Gedeveanishvili, S.; Deevi, S.C. Processing of iron aluminides by pressureless sintering through Fe + Al elemental route. *Mater. Sci. Eng.* **2002**, *325*, 163–176. [[CrossRef](#)]
13. Steffens, H.; Dammer, R.; Fischer, U. Post Treatment of Metal Matrix Composites by Hot Isostatic Pressing. *Surf. Eng.* **1988**, *4*, 39–43. [[CrossRef](#)]
14. Cherepova, T.; Dmitrieva, G.; Tisov, O.; Kindrachuk, M. Research on the properties of Co-TiC and Ni-TiC HIP-sintered alloys. *Acta Mech. Autom.* **2019**, *13*, 57–67. [[CrossRef](#)]
15. Zhang, H.; Wang, A.; Wen, Z.; Yue, Z.; Zhang, C. Effects of Hot Isostatic Pressing (HIP) on Microstructure and Mechanical Properties of K403 Nickel-based Superalloy. *High Temp. Mater. Process.* **2015**, *35*, 463–471. [[CrossRef](#)]
16. Gwyer, A.G. Über die legierungen des aluminiums mit kupfer, eisen, nickel, kobalt, blei und cadmium. *Z. Anorg. Chem.* **1908**, *57*, 113–153. [[CrossRef](#)]
17. Hall, R.C. Single crystal anisotropy and magnetostriction constants of several ferromagnetic materials including alloys of NiFe, SiFe, AlFe, CoNi, and CoFe. *J. Appl. Phys.* **1959**, *30*, 816–819. [[CrossRef](#)]
18. Zhu, S.M.; Tamura, M.; Sakamoto, K.; Iwasaki, K. Characterization of Fe<sub>3</sub>Al-based intermetallic alloys fabricated by mechanical alloying and HIP consolidation. *Mater. Sci. Eng. A* **2000**, *292*, 83–89. [[CrossRef](#)]
19. Bandyopadhyay, A.; Bose, S. *Additive Manufacturing*; Taylor & Francis Group: Boca Raton, FL, USA, 2020.
20. Gibson, I.; Rosen, D.; Stucker, B. *Additive Manufacturing Technologies*; Springer Science + Business Media: New York, NY, USA, 2010.
21. Kuryntsev, S. A review: Laser welding of dissimilar materials (Al/Fe, Al/Ti, Al/Cu)—Methods and techniques, microstructure and properties. *Materials* **2021**, *15*, 122. [[CrossRef](#)] [[PubMed](#)]
22. Watanabe, M.; Kumai, S.; Aizawa, T. Interfacial microstructure of magnetic pressure seam welded Al-Fe, Al-Ni and Al-Cu lap joints. In *Materials Science Forum*; Trans Tech Publications Ltd.: Freinbach, Switzerland, 2006; Volume 519, pp. 1145–1150.

23. Kokolis, J.; Chakmakchi, M.; Theocharopoulos, A.; Prombonas, A.; Zinelis, S. Mechanical and interfacial characterization of laser welded Co-Cr alloy with different joint configurations. *J. Adv. Prosthodont.* **2015**, *7*, 39–46. [[CrossRef](#)] [[PubMed](#)]
24. Loh, N.L.; Sia, K.Y. An overview of hot isostatic pressing. *J. Mater. Process. Technol.* **1992**, *30*, 45–65. [[CrossRef](#)]
25. European Powder Metallurgy Association. *Einführung in Die PM/HIP-Technologie*; European Powder Metallurgy Association: Brussels, Belgium, 2014.
26. Kallenbach, E.; Eick, R.; Quendt, P. *Elektromagnete*; B.G. Teubener: Stuttgart, Germany, 1994.
27. Hagl, R. *Elektrische Antriebstechnik*; Carl Hanser Verlag: München, Germany, 2021.
28. Schmidt, H. *Simulation von Elektromagneten mit FEMM und Modelica*; Carl Hanser Verlag: München, Germany, 2019.
29. Becker, R.; Döring, W. *Ferromagnetismus*; Julius Springer: Berlin, Germany, 1939.
30. Schatt, W.; Wieters, K.-P.; Kieback, B. *Pulvermetallurgie*; Springer: Berlin/Heidelberg, Germany, 2007.
31. WAB. Available online: <https://www.wab-group.com/de/mischtechnik/3d-schuettelmischer/produkt/turbula/> (accessed on 14 June 2022).
32. Schrüfer, E.; Reindl, L.; Zagar, B. *Elektrische Messtechnik: Messung Elektrischer und Nichtelektrischer Größen*; Carl Hanser Verlag: München, Germany, 2018.
33. ALUNOX Schweißtechnik GmbH. AX-5754 AX-ALMg3; ALUNOX Schweißtechnik GmbH: Willich, Germany, 2013.